JOURNAL OF CATALYSIS 65, 59–77 (1980)

Multiple Isotope Tracing of Methanation over Nickel Catalyst

J. HAPPEL,* I. SUZUKI,† P. KOKAYEFF,* AND V. FTHENAKIS*

* *Department of Chemical Engineering and Applied Chemistry, Columbia University, New York, New York 10027, and † Department of Chemistry, Utsunomiya University, 350 Mine, Utsunomiya, Japan*

Received September 27, 1979; revised January 15, 1980

The methanation of mixtures of carbon monoxide and hydrogen over a supported nickel catalyst was studied by transient isotopic tracing with ^{13}C, ^{18}O, and D. A mechanism is proposed based on computer modeling which takes into account results from a wide variety of data. Evidence is presented that rate controlling steps involve hydrogenolysis of chemisorbed CH_x species ($x = 0$–3) rather than only the splitting of carbon monoxide or the formation of an "enolic" intermediate. Carbon dioxide formation appears to occur directly rather than through the water gas shift reaction. The computer program enables estimates to be made of concentrations of intermediates as well as velocities of individual steps in the mechanism. Under reaction conditions predominant adsorbed species appear to be carbidic carbon plus hydrogenated hydrocarbon intermediates.

INTRODUCTION

We have studied a number of industrial reactions using commercial catalysts under steady-state reaction conditions in which superposed tracer transfer was also at steady state (*1*). Use of this technique often makes it possible to determine individual step velocities in a reaction mechanism when the overall reaction is reversible. It is not possible to determine the concentrations of surface intermediates, however.

Beginning in 1972 we extended steady-state isotope tracing to a technique using transient isotope superposition (*2*) and recently demonstrated its applicability in a study of the oxidation of carbon monoxide over Hopcalite catalyst (*3*). The elementary step velocities as well as surface concentrations for this reaction were estimated.

If a gradientless recirculating reactor is employed, the material balances representing isotopic transfer result in a system of simultaneous linear algebraic equations for steady-state isotopic transfer. In the case of transient tracing the redistribution of tracer is instead described by a set of simultaneous linear differential equations with constant coefficients. To our knowledge this technique has not been applied by other investigators to catalytic studies, though, of course, transient kinetic studies both with and without use of isotopic tracing are not new.

Mathematically such systems are analogous to networks of continuous stirred tank reactors or compartments. The number of compartments is equal to the number of terminal species and intermediates. The step velocities are represented by interconnection between them. Transient tracing using isotopes has been applied to physiological and biochemical systems and excellent reviews by Berman (*4–6*) discuss theory and applications of compartmental models in these fields. In biological systems radioactive tracers with high activity are usually introduced in small concentrations and the differential equations are linearized by taking advantage of the fact that a small perturbation of a nonlinear system behaves linearly (*6*). Our technique of superposition enables the transients to be described by linear differential equations without using small concentrations of tracer.

Recently Le Cardinal *et al.* (*7*) applied this superposition technique to homogeneous chemical reaction systems. Their paper was discussed further by Happel (*8*) and Le Cardinal (*9*). The form of equations given by Le Cardinal is not directly applicable to our studies since it involves no

0021-9517/80/090059-19$02.00/0

holdup of chemisorbed species on a solid catalyst. Le Cardinal's paper, also discusses some interesting aspects of the problem of identifiability of the parameters involved in a given model.

Another aspect of isotope kinetics is that the distinguishability of parameters is improved because a much richer collection of data is available and the correlating equations are simpler. A set of experiments is conducted at constant temperature, pressure, and concentrations of reacting species: This requires more experimentation to obtain a range of kinetic information, but the usual kinetic studies must generally deal with much more complicated sets of equations (*10, 11*).

A number of reviews are available discussing various aspects of the chemistry and mechanisms for catalytic methanation over various metals (*12–14*) using techniques other than those employed in this study. The overall reaction over nickel proceeds at a high rate and selectivity as follows:

$$CO + 3H_2 = CH_4 + H_2O. \quad (1)$$

However, CO_2 is also produced to a substantial degree as the ratio of H_2/CO in the reacting gases is reduced. This can be represented by a second reaction:

$$2CO + 2H_2 = CH_4 + CO_2. \quad (2)$$

Reaction (2) can be obtained by adding to reaction (1) the water gas shift reaction:

$$CO + H_2O = CO_2 + H_2. \quad (3)$$

Any two of the three reactions shown by Eqs. (1)–(3) may be chosen as independent reactions to predict equilibrium yields. This does not imply that the kinetics proceed first by reaction (1) followed by reaction (3). Ponec (*14*) concludes that CO_2 is produced directly by reaction (2) and our own studies, discussed later in this paper, support this.

Some studies have addressed the question of whether chemisorbed CO adds H_2 directly to form a hydroxy carbene or "enolic" type intermediate or whether it first dissociates to form an adsorbed carbon or carbidic species which subsequently reacts with hydrogen. The presence of H_2–CO surface complexes has not been observed by infrared spectroscopy (*15–18*) and other more recent research (*19–23*) lends great weight to the latter hypothesis.

Another unresolved question is the nature of the rate-determining step of the mechanism. Our studies support the proposal of Araki and Ponec (*20*) that it involves the hydrogenation of adsorbed carbidic or CH_x species rather than chemisorption of CO or the rate of initial intermediate formation whether it be enolic or carbidic. Our studies for the first time present clear evidence of the presence of surface hydrocarbon intermediates during methanation over nickel catalyst.

METHODS

Apparatus and Procedure

The apparatus employed in this study was a gradientless recirculating all-glass open flow reactor (*24*). It consists of a catalyst chamber, a magnetically activated piston pump, check valves, high-temperature solenoid coils, a recycle rotameter, and associated connecting tubing (see Fig. 1). The entire reactor was surrounded by a heater and the system has been operated at temperatures up to 480°C. Helium or hydrogen was used as a carrier gas. A feed gas mixture of hydrogen and carbon monoxide is injected into the system using 100-ml syringe pumps (Sage Instruments, Model 351).

Inlet and outlet gases were analyzed with a Finnigan quadrupole mass spectrometer (Type 1015C) with the electron energy fixed at 50 eV. The reaction system was connected to the spectrometer to either pass reactor effluent through P_2O_5 to remove water or to pass it directly into the spectrometer. For steady-state operation of unmarked gases the peak heights at $m/e = 15$, $m/e = 18$, $m/e = 28$, and $m/e = 44$ were

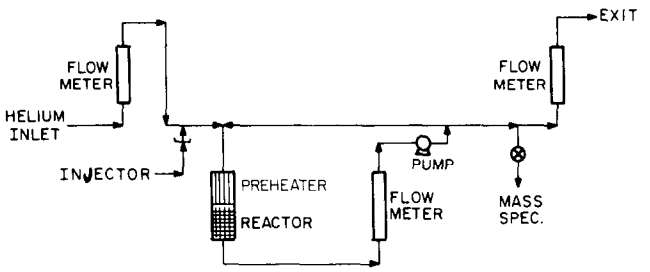

FIG. 1. Schematic diagram of recirculating reactor system.

used to obtain the realtive concentration of methane, water, carbon monoxide, and carbon dioxide respectively. These peak heights were proportional to the corresponding concentration when concentrations were less than 3% (v/v) when diluted with helium or hydrogen. A background peak at $m/e = 29$ was observed in the unmarked feed due to the natural abundance of ^{13}C (1.11%). The $m/e = 29$ peak was employed to determine the extent of ^{13}C marking in CO during tracer experiments, making suitable corrections for background and the operation of the helium separator. For $^{13}CH_4$ analysis, the peak height at $m/e = 17$ was employed with corrections. In some cases water was removed by P_2O_5 to check the analysis. $^{13}CO_2$ was analyzed by measurement of the peak height $m/e = 45$.

In each experiment the catalyst was heated at 480°C under a hydrogen flow for 2 hr before the run. Reactants were then introduced into the system with the syringe and steady state was usually attained within 1 or 2 hr. Then, the syringe feeding untagged compounds was replaced quickly with another syringe containing the tagged material. This procedure corresponded to a step function (step-up) of the tagged species in the reaction while the overall reaction was still steady. The increase in the tagged atoms in reactants and products was followed with the mass spectrometer.

Exceptions were made to this procedure in the qualitative experiments reported in Tables 1–6. For results reported in Tables 3 and 4 the reactor was operated partly as a closed system in an attempt to observe possible reverse reaction. In the deuterium tracing experiment reported in Table 5, hydrogen flow was completely replaced by deuterium.

Dead space in the reactor system was obtained by curve-fitting of the changes in $m/e = 28$ with time after step-function introduction of nitrogen into the system. This was checked by use of argon in place of nitrogen. It was assumed that rapid mixing occurred in the system. The result was checked by integration of the time curves as compared with the known rate of nitrogen introduction. The recirculation rate was approximately 3000 ml/min. Calculations indicate that with the very low reaction rate and dilute mixtures employed interphase and intraphase concentration and temperature gradients are negligible. In the studies reported here the dead volulme $\beta =$ 206.1 ml in all cases.

In reporting tracer levels, in all cases the definition of tracer level z^i following Eq. (4) was employed. Thus for deuterium tracing, for example,

$$z^{H_2} = \frac{\text{concn of } D_2 + \frac{1}{2} \text{ concn of HD}}{\text{concn } D_2 + \text{concn } H_2 + \text{concn HD}}.$$

Generally operation was conducted at atmospheric pressure. Temperature of operation is noted in individual experiments and was usually not far above 200°C. This temperature was chosen to obtain convenient rates of reaction for observation of tracer transients.

The catalyst used was nickel supported on kieselguhr supplied by Harshaw Chemi-

cal Company H104T (60 wt% Ni), crushed and screened to 30–60 mesh size. In all the present studies the same initial charge of catalyst weighing 0.744 g was used. Hydrogen (99.9999% pure), deuterium (99.5% pure), helium (99.999% pure), methane (99.97% pure), and carbon monoxide (99.99% pure) were obtained from Matheson Gas Company. Perdeuteromethane CD_4 (99% pure) and tagged methane $^{13}CH_4$ (90% pure) were obtained from Stohler Isotope Chemicals Company. Heavy water D_2O (99.8% pure), tagged carbon monoxide ^{13}CO (98.7% pure), and tagged carbon monoxide $C^{18}O$ (99% pure) were obtained from Bio-Rad Laboratories. All components were used without further purification for preparing feed mixtures.

Method of Correlation

The data obtained in the quantitative experiments consist of the overall steady rates of product formation from the feed gas together with the transient fractional markings. A nonlinear least-squares regression technique (*3*) is employed for computer analysis of the fit of various mechanistic models to the data. The unknown parameters to be found for each postulated model can be expressed by a set of simultaneous linear differential equations with constant coefficients. These parameters consist of the concentrations of chemisorbed intermediates together with reverse velocities of those mechanistic steps which are not unidirectional or at equilibrium.

The system to be modeled is assumed to consist of a number of cells or compartments involving each of the reacting species which can interact with each other. It is assumed that the gas phase is completely mixed and that all surface sites of a given chemisorbed species on the catalyst are equally accessible. In order for the overall reaction in a recirculating reactor system to be at the steady-state condition feed must be continuously introduced and product withdrawn.

Then at time $t = 0$, a known concentration of a tagged atomic species i is substituted in one or more of the feed streams at concentration z_F and is maintained at a constant value. There will be n species containing the same kind of atoms as the tagged atom. For this step-function input of marked atoms n differential equations can be written corresponding to material balances for each of the n species:

$$\frac{dz_p}{dt} = Az_p + b, \tag{4}$$

where

z_p^i = a vector giving fractional tagging of i in each of $j = 1, \ldots, n$ species,
= (atoms of isotope of i per mole of j)/(total atoms of i per mole of j),

A = an $n \times n$ matrix consisting of coefficients involving the parameters in the material balances,

b = an n vector determined from the input of tracer in the feed, which is taken as constant in marked species.

Note that z_p is not taken as the *amount* of tracer in each compartment but as the *fractional* marking obtained by substitution of marked species for unmarked species in the reacting system. Also in heterogenous systems containing a fixed catalyst bed the A matrix elements which involve chemisorbed species will not include the residence time as required for the moving fluid.

Regarding the n compartments for a given tracer atom, species required in the overall reaction mechanism which do not contain this atom will, of course, not be traced and will not appear in that set of differential equations. On the other hand, if atoms are present in the catalyst which can exchange with the tracer, even though they do not enter into the overall reaction being modeled, additional compartments must be added to allow for such exchange. Similar considerations apply if tracer elements can be transferred from reacting species to products by other paths than the mechanism being modeled.

In developing Eq. (4) it is assumed that the marked atoms are indistinguishable in kinetic behavior from those which are unmarked. No isotope kinetic effects are considered and all the same kind of marked atoms in a molecular species are assumed to react with the same velocity as those that are unmarked.

The form of Eq. (4) is especially convenient for computer solution but it may in some cases prove convenient to use more complicated modeling. Thus, instead of the constant vector **b**, one might introduce feed components in a time-dependent fashion.

Also where more than one marked atom is present in a molecule for given terminal species, even if all the atoms are structurally equivalent, it may be desirable to follow the distribution of marking as well as the total fractional marking as is done in Eq. (4). This would be required, for example, to take full advantage of deuterium tracing of the methanation reaction. In this case the differential equations are still first order though no longer linear.

The problem to be solved when one has derived the appropriate equations is not in finding their solution but rather in determining the unknown coefficients or elements of the **A** matrix given a set of experimental values of z_p over a period of time. This is a parameter estimation problem that must be solved by nonlinear programming methods. Details of the procedure we used for this purpose are given by Happel *et al.* (*3*).

From the mathematical standpoint one identifies the model by a number of pools and their interconnections. Information about the nature of the material in compartments and their interaction may come from other sources in addition to transient tracing experiments such as steady-state tracer measurements, a priori information about the existence or nonexistence of certain pathways or intermediates, and information developed by methods of surface examination during reactions such as various spectroscopic observations. A given mathematical model may be consistent with more than one assumed mechanism if the contents of all compartments cannot be completely identified.

The computational procedure which we have employed includes a statistical treatment which provides information on goodness of fit, based on average deviation of predicted from actual data, expected deviation of determined parameters, and degree of correlation among them. In addition to these criteria the predicted and calculated data are plotted to observe the possible presence of systematic deviations.

RESULTS

Preliminary Experiments

Tests thus far have been conducted on a typical commercial nickel catalyst, Harshaw 104T. Professor A. L. Dent of Carnegie–Mellon University kindly measured surface characteristics. The total area of the catalyst is 87 m^2/g, which we checked. Hydrogen uptake at 100°C is 7.10 ml/g (317 μmole/g). Taking the area occupied by a hydrogen molecule as 13.44 $Å^2$ (*25*) we find a total area of active nickel surface equal to 25.6 m^2/g. We observed rates of methanation for 3/1 H_2/CO ratio mixtures at 20 Torr hydrogen partial pressure in helium carrier gas at 275°C. A methane turnover number (reactions/sec · site) equal to 0.41×10^{-3} was obtained. This rate is close to that reported over several nickel catalysts by Goodman *et al.* (*26*), confirming the generally accepted finding that these catalysts are not structure sensitive for the methanation reaction.

Following this, we conducted steady-state experiments to determine the effect of variation in pressure of carbon monoxide and hydrogen on reaction rate. The rate of methanation at 205°C was found to be directly proportional to hydrogen partial pressure and inversely proportional to that of carbon monoxide, roughly in agreement with the literature.

We also conducted some transient exper-

iments without tracer in a manner somewhat similar to the study of methanation over an iron catalyst reported by Matsumoto and Bennett (*27*). In one series, data for which are shown in Table 1, a H_2/CO mixture of 3.5/1 diluted with helium was passed over the catalyst for a period of 140 min in a recirculating reactor until steady state was obtained. At that time the H_2/CO flow was abruptly stopped but helium flow was continued. Analysis of the data indicates that as soon as helium was introduced little further reaction with ambient CO and H_2 occurred and they were rapidly flushed from the system. During the period from 140 to 265 min methane, hydrogen, and water were desorbed in appreciable amounts. Allowing for the material originally present in the dead space, it is estimated that during this period recoveries of CH_4 and H_2O were, respectively, 1.08 and 0.71 ml/g of catalyst. These observations are in contrast to results with iron catalyst reported by Matsumoto and Bennett who observed no methane desorption in their experiments in which helium alone was passed over the catalyst after steady state was obtained. Perhaps chemisorbed hydrogen reacted to form methane in our experiments.

The experiments shown in Table 1 were continued by switching from helium to hydrogen after 265 min (i.e., after passing helium over the catalyst for 125 min following attainment of steady state by 140 min of original operation) and this hydrogen injec-

TABLE 1

Transient Desorption Experiments

Reaction temperature = 233°C.

At time $t = 0$, a mixture of CO of 0.221 ml/min and of H_2 equal to 0.771 ml/min was flowed over the catalyst. He carrier gas was introduced at a rate of 75.5 ml/min.

At time $t = 140$ min flow of CO and H_2 was stopped. Helium carrier flow was continued up to 265 min.

At time $t = 265$ min, hydrogen flow was resumed at 0.80 ml/min. Helium carrier flow was continued throughout the run.

The following data were obtained throughout these three modes of operation:

Time (min)	CO (ml/min)	H_2 (ml/min)	CH_4 (ml/min)	H_2O (ml/min)
55	0.152	0.570	0.076	0.049
80	0.133	0.514	0.096	0.065
105	0.130	0.511	0.098	0.064
130	0.123	0.476	0.106	0.063
140	0.127	0.504	0.101	0.065
141	0.087	0.363	0.088	0.059
142	0.054	0.194	0.070	0.055
143	0.036	0.128	0.059	0.047
144	0.029	0.126	0.055	0.044
145	—	0.108	0.048	0.033
146	0.015	0.087	0.036	0.023
148	0.013	0.064	0.034	0.019
152	0.010	0.060	0.025	0.009
155.5	0.008	0.053	0.016	0.007
160	0.006	0.044	0.011	0.004
171	0.001	0.036	0.014	0.004
190	0.000	0.030	0.002	0.003
213	0.000	0.028	0.001	0.000
265.5	—	—	0.671	—
266	—	0.17	0.118	0.025
267	—	0.15	0.168	0.040
267.5	—	—	0.180	0.042
268.5	—	—	0.180	—
269	—	0.29	0.142	0.044
272	—	0.33	0.092	0.022
278	—	0.55	0.048	0.014
291	—	0.77	0.018	0.005
310	—	0.74	0.005	0.005
330		0.80	0.003	0.000

TABLE 1—*Continued*

Some CO_2 determinations were also made but are not reported since they varied erratically.

From these data it is estimated that the following net recoveries were obtained during the helium desorption and subsequent hydrogen reaction periods allowing for material contained in the dead space:

	Gas production (ml/g catalyst at standard conditions (NTP))	
	Helium desorption (140–265.5 min)	Hydrogen reaction (265.5–330 min)
CO	0.17	—
H_2	3.2	−9.7[a]
CH_4	1.08	3.3
H_2O	0.71	0.76

[a] Hydrogen converted by reaction or adsorption.

tion was continued an additional 65 min. It is estimated that during this period 9.7 ml/g of hydrogen reacted with material present on the catalyst or was adsorbed. At the same time 3.3 ml/g of CH_4 was recovered, along with 0.7 ml/g of H_2O. CO_2 recovery was very small. In view of the inaccuracy of hydrogen analysis and consequent difficulty in obtaining an exact figure for the amount of hydrogen adsorption, the results seem to be consistent with the hypothesis that a carbonaceous deposit on the catalyst is subsequently hydrogenated to produce methane.

Irreversible Steps

The overall reactions represented by Eqs. (1) and (2) are essentially irreversible under reaction conditions (at 200°C, $K_p = 2.17 \times 10^{11}$ and 4.94×10^{13}, respectively (*28*)) and therefore there must be at least one irreversible step in the reaction mechanism.

In order to determine whether the slow step occurs in the path of carbon transfer an experiment was conducted (Table 2) by introducing $^{13}CH_4$ into a recirculating reaction system in which unmarked CO and H_2 were reacting to produce methane. Only a very small amount of ^{13}CO was detected in the effluent so an irreversible step exists in the carbon transfer path.

TABLE 2

Steady-State $^{13}CH_4$ Marking Experiment

Reaction temperature = 222°C
He flow rate = 55.4 m/min (NTP)

	Inlet rate (ml/min)	Outlet rate (ml/min)
CO	0.118	0.089
H_2O	0.016	0.066
H_2	0.750	0.652
CH_4	0.125	0.149
CO_2	—	0.005

Marking of inlet CH_4, fraction of $^{13}CH_4$, $z^{CH_4} = 0.23$.
Marking of exit CO, fraction of ^{13}CO, $z^{CO} = 0.001$.

TABLE 3

Forward Transfer of Deuterium to CH_4 in Absence of CO

Reaction temperature = 228°C
Inlet deuterium flow rate = 42.8 ml/min (NTP)
Inlet methane flow rate = 2 ml/min (NTP)

Time (min)	Deuterated methane produced (%)				
	CH_4	CH_3D	CH_2D_2	CHD_3	CD_4
	Reactor operated with open flow				
0	100	0	0	0	0
50	99.0	1.0	0	0	0
	Reactor operated closed with same initial feed composition				
0	100	0	0	0	0
70	93.8	5.1	1.1	0	0
140	86.5	12.2	1.1	0	0

The product gas was passed through P_2O_5 before analysis so HDO, H_2O, and D_2O were not determined. CO_2 was absent from the product.

To test for the irreversibility of hydrogen transfer similar experiments were performed with deuterium marking. Table 3 gives results of an experiment in which mixture of CH_4 and D_2 was passed over the catalyst. At 230°C less than 1% marking of the methane to produce CH_3D was observed after 50 min. Less than 13% exchange of CH_4 with D_2 was observed even after 140 min of recirculation with the system closed.

Another experiment (Table 4) explored the rate of transfer of deuterium from CD_4 to H_2 in both the presence and absence of CO. Only a very small amount of deuterium was transferred. There was again very little increase when the system was operated as a closed reactor.

Transient Tracing

In order to obtain further information on the nature of the CH_x intermediates a step-function superposition experiment was conducted in which a steady state was first reached in a recirculating reactor system, using a high feed ratio of hydrogen to CO.

TABLE 4

Transfer of Deuterium from CD_4 to H_2

Reaction temperature = 214°C Reactor operated with open flow				
Feed			Time (min)	Outlet H_2 fractional marking (z^{H_2})
CO (ml/min)	CD_4 (ml/min)	H_2 (ml/min)		
0	0.5	51.9	0	1×10^{-5}
			60	2×10^{-5}
0.5	0.5	51.9	0	1×10^{-5}
			60	2×10^{-4}

Reactor operated closed				
Gaseous content (partial pressure)			Time (min)	Outlet H_2 fractional marking (z^{H_2})
P_{CO} (atm)	P_{CD_4} (atm)	P_{H_2} (atm)		
0	0.0095	0.991	0	1×10^{-5}
			100	3×10^{-5}
0.0095	0.0095	0.981	0	1×10^{-5}
			60	2×10^{-4}

In this experiment no helium carrier was employed and no CO_2 production was observed. After reaching steady state, hydrogen was replaced by deuterium, all other conditions remaining the same. Details of the experimental conditions are given in Table 5 and the appearance of deuterated CH_xD_{4-x} is reproduced in Fig. 2. Distribution of deuterium in the product species is not random but exact modeling is not possi-

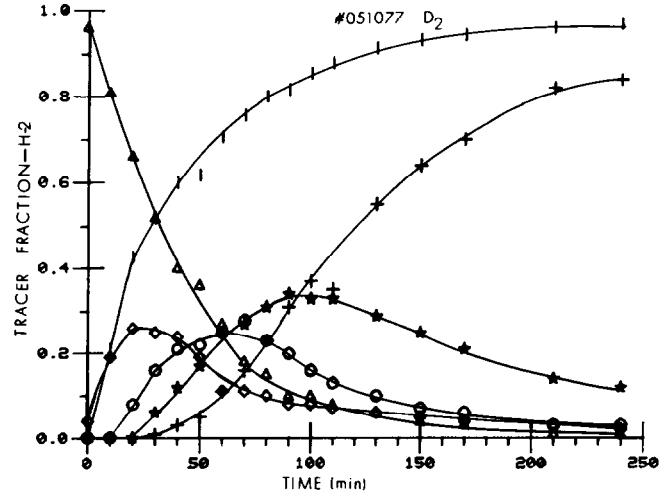

FIG. 2. D_2 tracing: Ni catalyst. (|), z^{D_2}; (△), z^{CH_4}; (◇), z^{CH_3D}; (○), $z^{CH_2D_2}$; (★), z^{CHD_3}; (+), z^{CD_4}. Run No. 051077; T = 253°C; feed molal ratio, H_2/CO = 20/1.

TABLE 5

D_2 Step-Function Experiment

Reaction temperature = 253°C
Weight of catalyst = 0.346 g (only in this run)

	Initial conditions	
	Inlet flow rate (ml/min)	Outlet flow rate (ml/min)
CO	1.0	0.894
H_2	19.7	19.38
H_2O	0.015	0.121
CH_4	0	0.102

Deuterium flow of 19.7 ml/min replaced hydrogen flow at zero time.

Time (min)	Fraction of deuterium in $H_2 + D_2 + HD$ (z^{H_2})	Observed distribution in product: Fraction of each CH_xD_{4-x} species of total				
		CH_4	CH_3D	CH_2D_2	CHD_3	CD_4
0	0.002	0.96	0.04	0	0	0
10	0.210	0.81	0.19	0	0	0
20	0.427	0.66	0.26	0.08	0	0
30	0.519	0.52	0.25	0.16	0.06	0.01
40	0.600	0.40	0.24	0.21	0.12	0.03
50	0.617	0.36	0.19	0.22	0.17	0.05
60	0.706	0.27	0.11	0.25	0.25	0.11
70	0.756	0.18	0.11	0.28	0.27	0.16
80	0.801	0.15	0.08	0.23	0.31	0.23
90	0.817	0.10	0.05	0.20	0.34	0.31
100	0.854	0.10	0.04	0.16	0.33	0.37
110	0.880	0.08	0.01	0.13	0.33	0.35
130	0.912	0.06	0	0.10	0.29	0.55
150	0.931	0.04	0	0.07	0.25	0.64
170	0.944	0.03	0	0.06	0.21	0.70
210	0.960	0.01	0	0.03	0.14	0.82
240	0.967	0.01	0	0.003	0.12	0.84

ble because of isotopic kinetic effects which have not as yet been resolved. However, the relatively short delay time in appearance of CH_3D as compared with that of more highly deuterated species indicates that partially hydrogenated adsorbed intermediates are being deuterated.

Another deuterium tracing experiment was conducted in a manner following somewhat the procedure of the previous desorption experiments without tracer outlined in Table 1. Details of this experiment are given in Table 6. Steady state in a recirculating reactor was first reached by operation for 120 min. A feed of H_2/CO ratio of 8/1 was employed in a helium carrier and very little CO_2 was produced. Following this, the feed of hydrogen and CO was stopped and helium flow was continued for an additional period of 276 min. Results were somewhat similar to those obtained previously except that recoveries of adsorbed gases were somewhat higher, possibly due to the higher partial pressure of feed components. At this point deuterium was introduced into the helium carrier instead of hydrogen, as was done previously.

The predominant product during this deuterium injection period was CD_4 evidently produced by deuteration of carbidic carbon which was not removed by helium flushing. No CH_4 was produced, indicating

TABLE 6

D_2 Desorption Experiment

Reaction temperature = 226°C

	Initial conditions Inlet flow rate (ml/min (NTP))	Outlet flow rate (ml/min (NTP))
CO	0.60	0.40
CO_2	0	0.004
H_2	4.80	—
H_2O	0.023	0.21
CH_4	0	0.19
He	37.2	0

After 120 min, helium alone was passed over the catalyst for an additional period of 276 min. This resulted in recovery of CO, CH_4, and H_2O of 0.82, 2.84, and 2.83 ml/g of catalyst, respectively. Traces of CO_2 were also produced.

Following this, 0.6 ml/min of deuterium was introduced into the helium feed which was maintained constant. The following rates of production of hydrocarbon species were observed, starting at zero time beginning with deuterium injection.

Time (min)	Production rate of CH_xD_{4-x} species (ml/min)			
	CD_4	CHD_3	CH_2D_2	CH_3D
2	0.000	0.000	0.000	0.000
3	0.000	0.000	0.001	0.001
5	0.002	0.000	0.004	0.003
7	0.004	0.003	0.006	0.003
9	0.008	0.010	0.007	0.004
14	0.017	0.010	0.008	0.003
19	0.022	0.006	0.007	0.003
30	0.024	0.001	0.005	0.002
50	0.019	0.000	0.002	0.001
83	0.012	0.000	0.001	0.000
133	0.012	0.000	0.000	0.000

These rates correspond to the following total production in ml/g of catalyst:

CD_4	1.99
CHD_3	0.12
CH_2D_2	0.30
CH_3D	0.12
Total	2.53

No CH_4 or D_2O could be detected in the product.

that the species CH_4l is not present. The most abundant partially deuterated species was CH_2D_2, which might be taken as an indication that the predominant hydrocarbon intermediate is adsorbed CH_2l. Roughly equal proportions of CHD_3 and CH_3D were recovered, possibly due to a rearrangement of chemisorbed CH_x species:

$$2CH_2l + l \rightarrow CH_3l + CHl. \quad (5)$$

Actually a somewhat greater proportion of CH_2D_2 is indicated than corresponds to equilibrium for this reaction but since the partially deuterated methane production is relatively small these findings must be confirmed.

^{18}O Transient Superposition Tracing

While deuterium tracing is useful in following the steps in methanation involving hydrocarbons, it is not as readily employed for tracing the path of hydrogen to water. Deuterium exchanges rapidly with hydrogen and with water following reaction mechanisms different from those involved in methanation. It was thought that the employment of ^{18}O would be useful in following the role of H_2 and CO of removing oxygen produced by CO dissociation.

Details of a transient experiment for this purpose conducted by incorporating a step change from unmarked CO to $C^{18}O$ in a low H_2/CO ratio feed are given in Table 7. The appearance of ^{18}O in H_2O and CO_2 was observed. Figure 3 shows the appearance of marking during a period of time following injection of tracer. Marking in CO_2 occurs somewhat more rapidly than in H_2O, indicating that surface oxygen produced by dissociation of CO is being directly converted to CO_2 by further reaction with CO rather than by reaction with water. In this experiment $C^{18}O$ concentration approached the feed concentration in about 20 min but neither CO_2 nor H_2O marking reached steady state after twice that period of time. Thus it is possible that oxygen in the silica support can exchange with these components.

Several mechanisms were employed in

TABLE 7

$C^{18}O$ Step-Up Experiment

Pressure = 1 atm
Temperature = 231°C
Helium flow rate = 17.89 ml/min

	Inlet rate (ml/min)	Outlet rate (ml/min)
CO	0.59	0.45
H_2O	0.049	0.17
H_2	1.80	1.43
CH_4	—	0.124
CO_2	—	0.010
	CO conversion	22.9%
	CO conversion to CH_4	21.20%
	CO conversion to O_2	1.70%

Initial tracing level = z_i^{CO} = 13.2% of ^{18}O

Computed parameters	
$C^{COl} + C^{O}$ (ml/g)	0 ± 0.10
C^{Os} (ml/g)	11.1 ± 2.5[a]
Rate of O exchange with H_2O, v_5 (ml/g/min)	0.35 ± 0.04[a]
Rate of O exchange with CO_2, v_6 (ml/g/min)	0.008 ± 0.001[a]

[a] Calculated on basis of equivalent volumes of atomic oxygen.

computer modeling with oxygen atoms in H_2O and CO_2 participating in an exchange reaction with a pool of lattice oxygen Os. It is possible that more elaborate models would be useful, if the data could be taken with greater accuracy. The model employed here was the following:

$$\begin{aligned}
&CO + l \underset{v_{-1}}{\overset{v_{+1}}{\rightleftharpoons}} COl,\\
&COl + l \xrightarrow{v_{+2}} Cl + Ol,\\
&Ol + H_2 \xrightarrow{v_{+3}} H_2O + l,\\
&Ol + CO \xrightarrow{v_{+4}} CO_2 + l,\\
&H_2O \overset{v_5}{\rightleftharpoons} Os\\
&CO_2 \overset{v_6}{\rightleftharpoons} Os
\end{aligned} \tag{6}$$

where l represents surface sites for adsorption of reaction with the catalyst, s refers to inactive sites with which oxygen in CO_2 or H_2O can exchange. Reaction Step 1 is at equilibrium and occurs rapidly. Step 2 is taken as unidirectional and Ol is taken as very small, so delay time in appearance of ^{18}O in the product is small. Steps 3 and 4 are taken as unidirectional. In the case of the exchange reactions given in steps 5 and 6, the reaction is at equilibrium but the rate of exchange may be slow relative to the overall rate given by $v_2 = v_{+3} = v_{+4}$, as contrasted with the rapid reaction rate of the velocity $v_{\pm 1}$ for step 1. Equation (6) may be represented by the compartmental model given in Fig. 4, which involves four parameters, two pools (COl) and O_s), and the exchange velocities v_5 and v_6. Material balances for ^{18}O tracer transfer may be written for CO, H_2O, CO_2, and O_s corresponding to rates of reaction per unit weight of catalyst. These equations are as follows, in the form of Eq. (4):

$$\frac{dz^{CO}}{dt} = \frac{(V + V' + F_0^{CO}/W)}{(\beta C_C^{CO}/W + C^{COl})} z^{CO} + \frac{F_i^{CO} z_i^{CO}}{(\beta C^{CO}/W + C^{COl})}, \tag{7}$$

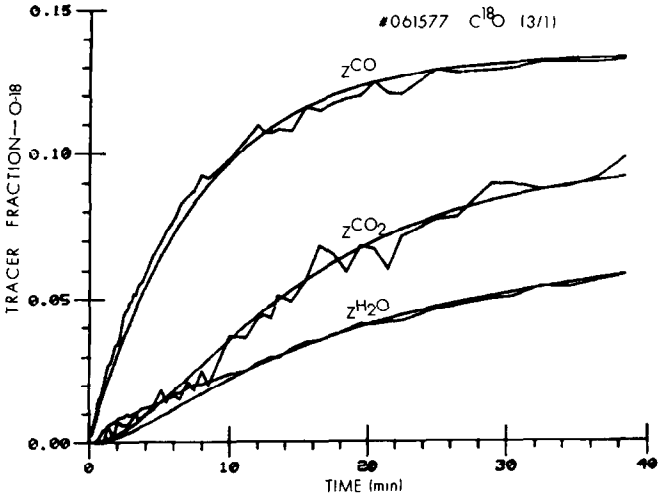

FIG. 3. $C^{18}O$ tracing: Ni catalyst. Smooth curve represents theoretical results. Uneven curve represents data. Run No. 061577; feed molal ratio, $H_2/CO = 3/1$.

$$\frac{dz^{H_2O}}{dt} = \frac{(V + V')}{\beta C^{H_2O}/W}(z^{CO} - z^{H_2O}) + \frac{v_5}{\beta C^{H_2O}/W}(z^{O_s} - z^{H_2O}), \quad (8)$$

$$\frac{dz^{CO_2}}{dt} = \frac{V'}{\beta C^{CO_2}/W}(z^{CO} - z^{CO_2}) + \frac{v_6}{\beta C^{CO_2}/W}(z^{O_s} - z^{CO_2}), \quad (9)$$

$$\frac{dz^{O_s}}{dt} = \frac{v_5}{C^{O_s}}(z^{H_2O} - z^{O_s}) + \frac{v_6}{C^{O_s}}(z^{CO_2} - z^{O_s}), \quad (10)$$

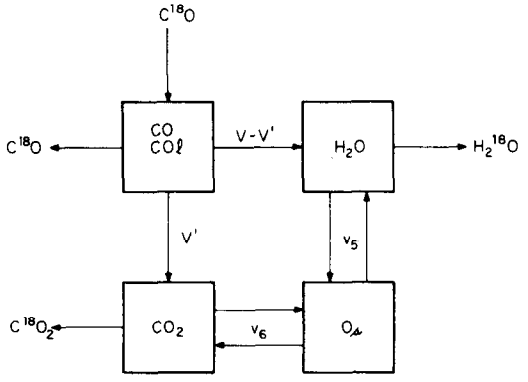

FIG. 4. $C^{18}O$ tracing: compartmental model.

where

C^{CO}, C^{CO_2}, C^{H_2O} = concentration of gas phase CO, CO_2, and H_2O in the reaction system,

C^{O_s} = concentration of exchangable oxygen on inert sites per unit weight of solid catalyst,

F_i^{CO}, F_0^{CO} = inlet and outlet flow rates of CO,

t = time following initial change to isotopically marked $C^{18}O$,

V = rate of production of CH_4 per unit weight of catalyst,

V' = rate of production of CO_2 per unit weight of catalyst,

v_5 = rate of exchange of oxygen atoms in water with inert catalyst sites,

v_6 = rate of exchange of oxygen atoms in CO_2 with inert catalyst sites,

W = total weight of catalyst within system,

β = volume of dead space,

z^j = fraction of ^{18}O in total oxygen content of components j = CO, H_2O, CO_2, in product streams

z_i^{CO} = fraction of ^{18}O in total oxygen content of feed CO stream,

z^{OS} = fraction of ^{18}O in total oxygen contained on inert catalyst sites.

In setting up these equations we employ the relationships $V - V' = v_{+3}$ and $V' = v_{+4}$.

Results of parameter estimation are listed in Table 7. The surface concentration of $COl + Ol$ is too low to be measured accurately by the modeling procedure (<0.1 ml/g catalyst). The value of the oxygen exchange capacity expressed as volume of equivalent atomic oxygen is 11.1 ml/g of catalyst (NTP), somewhat larger than the usual chemisorption quantities. Figure 3 gives a comparison of the experimental points with those predicted by the model.

^{13}C Transient Superposition Tracing

Results of ^{13}C tracing are most satisfactory because they do not present problems of isotopic kinetic effects or lattice exchange. A series of runs was made using step up changes in the ^{13}CO feed. Four of these experiments were conducted at high H_2/CO ratios in which no detectable CO_2 production occurred. Two experiments were conducted at lower ratios. It was found possible to correlate the ^{13}C transient data by a single mechanistic model consistent with other experiments thus far reported using D and ^{18}O as follows:

$$\begin{aligned}
&CO + l \underset{v_{-1}}{\overset{v_{+1}}{\rightleftharpoons}} COl,\\
&COl + l \overset{v_{+2}}{\rightarrow} Cl + Ol,\\
&Cl + H_2 \overset{v_{+3}}{\rightarrow} CH_2l,\\
&CH_2l + H_2 \overset{v_{+4}}{\rightarrow} CH_4 + l,\\
&CO + Ol \underset{v_{-5}}{\overset{v_{+5}}{\rightleftharpoons}} CO_2 + l,\\
&CO_2 + m \underset{}{\overset{v_6}{\rightleftharpoons}} CO_2m,
\end{aligned} \tag{11}$$

where l represents surface sites for adsorption or reaction with the catalyst, and m represents sites on which molecular CO_2 can exchange with the catalyst. As in the case of oxygen tracing, step 1 is assumed to be rapid and at equilibrium.

The corresponding compartmental model is given in Fig. 5. The model corresponds to five pools and requires the determination of the following five unknown parameters: three pools (C^{COl}), ($C^{Cl} + C^{CH_2l}$), (C^{CO_2m}); the velocity v_{-5}; and the exchange velocity v_6. For high ratio H_2/CO feeds no CO_2 is produced and only two parameters (C^{COl}) and ($C^{Cl} + C^{CH_2l}$) are required.

Material balances for ^{13}CO tracer transfer

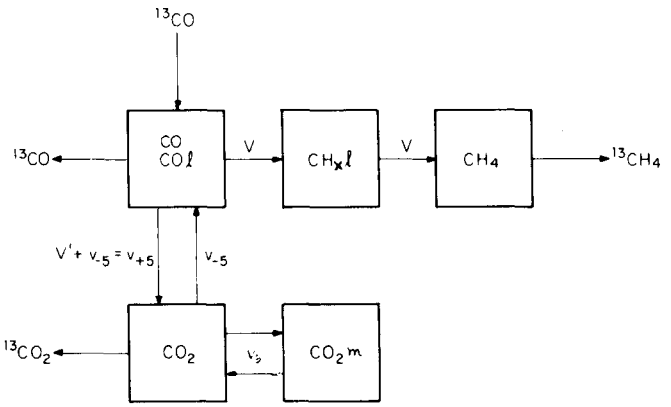

FIG. 5. ^{13}CO tracing: compartmental model.

may be written for CO, CH_xl, CH_4, CO_2, and CO_2m corresponding to rates of reaction per unit weight of catalyst. These equations are as follows, in the form of Eq. (4). In writing these balances, it is assumed that one of the CH_xl species, probably Cl, is present in much greater proportion than the remaining species which we have called CH_2l for simplicity until a more exact identification is possible.

$$\frac{dz^{CO}}{dt} = \frac{-(V + V' + F_0^{CO}/W + v_{-5})z^{CO}}{(\beta C^{CO}/W + C^{COl})} \frac{v_{-5}z^{CO_2}}{(\beta C^{CO}/W + C^{COl})} + \frac{F_i^{CO}z_i^{CO}}{(\beta C^{CO}/W + C^{COl})}, \quad (12)$$

$$\frac{dz^{(CH_xl)}}{dt} = \frac{V}{C^{(CH_xl)}}(z^{CO} - z^{CH_xl}), \quad (13)$$

$$\frac{dz^{CH_4}}{dt} = \frac{V}{\beta C^{CH_4}/W}(z^{CH_xl} - z^{CH_4}), \quad (14)$$

$$\frac{dz^{CO_2}}{dt} = \frac{(V' - v_{-5})}{\beta C^{CO_2}/W}(z^{CO} - z^{CO_2}) + \frac{v_6}{\beta C^{CO_2}/W}(z^{CO_2m} - z^{CO_2}), \quad (15)$$

$$\frac{dz^{CO_2m}}{dt} = \frac{v_6}{C^{CO_2m}}(z^{CO_2} - z^{CO_2m}), \quad (16)$$

where

C^{CO}, C^{CH_4}, C^{CO_2} = concentration of gas phase CO, CH_4, and CO_2,

C^{CH_xl}, C^{COl} = concentrations of chemisorbed COl and ($CH_xl = Cl + CH_2l$) on catalyst sites per unit weight of catalyst,

F_i^{CO}, F_0^{CO} = inlet and outlet flow rates of CO,

t = time following initial change to isotopically marked ^{13}CO,

V = rate of production of CH_4 per unit weight of catalyst,

V' = rate of production of CO_2 per unit weight of catalyst,

v_{-5} = rate of dissociative readsorption of CO_2 per unit weight of catalyst,

v_6 = rate of exchange of CO_2 per unit weight of catalyst,

W = total weight of catalyst in the system,

β = volume of dead space,

z^i = fraction of ^{13}C in total carbon content of component i = CO, CH_2l, CH_4, CO_2, or CO_2m,

z_i^{CO} = fraction of ^{13}CO in total carbon content of feed CO stream.

In setting up these equations we employ the relationships $V = v_{+2}$, v_{+3} and v_{+4}, $V' = v_{+5} - v_{-5}$.

Table 8 gives the results of six experiments using this model. A comparison of predicted output with actual tracer output for the four high H_2/CO ratio experiments is given in Figs. 6–9. Results for the two low H_2/CO ratio runs are given in Figs. 10 and 11. The parameters v_{+5} gave satisfactory fit for a range of values of methanae adsorption steps, so these values are not well determined. These curves are not simply an empirical best fit drawn through the data but involve the combination of exponentials which results from simulation of the chosen model. Runs were taken over a period of time with some variation in catalyst age and operating conditions.

All the data correspond to the same model. More than two unidirectional steps with appreciable surface concentrations preceding each step result in much more delay in appearance of ^{13}C in methane than is indicated by the data. However additional unidirectional steps preceded by relatively small amounts of adsorbed species will not result in increased delay. This requires that only one of the adsorbed CH_x

TABLE 8

^{13}CO Step-Up Experiments

	Pressure = 1 atm		
Feed mix ratio H_2/CO	91.3	64.1	26.0
Temperature (°C)	175	176	220
Inlet marking (z in CO[a])	0.068	0.145	0.087
Inlet CO feed (ml/min (NTP))	0.50	0.80	1.50
Inlet He (ml/min (NTP))	0	0	0
Rate to CH_4, V (ml/min/g)	0.22	0.27	0.71
Net rate to CO_2, V' (ml/min/g)	—	—	—
Computed parameters			
$C^{C} + C^{CO}$ (ml/g)	1.99 (±0.06)[b]	1.57 (±0.06)	0.00 (±0.06)
C^{CH_2} (ml/g)	2.32 (±0.05)	4.26 (±0.07)	2.23 (±0.04)
Feed mix ratio H_2/CO	17.5	4.0	3.0
Temperature (°C)	217	258	276
Inlet marking (z in CO)	0.128	0.106	0.106
Inlet CO feed (ml/min (NTP))	2.00	0.60	0.75
Inlet He (ml/min (NTP))	0	55.2	69.1
Rate to CH_4, V (ml/min/g)	0.88	0.119	0.177
Net rate to CO_2, V' (ml/min/g)	—	0.021	0.072
Computed parameters			
$C^{C} + C^{CO}$ (ml/g)	0.00 (±0.14)	0.38 (±0.04)	0.03 (±0.11)
C^{CH_2} (ml/g)	3.30 (±0.08)	0.97 (±0.02)	0.59 (±0.02)
Rate of CO_2 adsorption, v_{-5} (ml/min/g)	—	0.02 (±0.01)	0.30 (±0.06)
Rate of CO_2 production, v_{+5} (ml/min/g)	—	0.04 (±0.01)	0.37 (±0.06)
$C^{CO_2(s)}$ (ml/g)	—	0.10 (±0.02)	0.67 (±0.13)
Rate of CO_2 exchange, v_6 (ml/min/g)	—	0.02 (±0.01)	0.70 (±0.33)

[a] Values corrected for natural abundance of ^{13}C (1.11%) in unmarked CO. Plots at $t = 0$ start at zero initial marking.

[b] Values in parentheses are computed estimates of standard errors.

species must predominate. If relatively equal proportions of all were present larger delay times in appearance of ^{13}C in methane would result. In all cases the concentration of adsorbed carbonaceous CH_xI is higher than that of the equilibrium pool COI.

DISCUSSION

A tentative mechanism for the overall reaction system is obtained by combining step 3 of Eq. (6) with steps 1–5 of Eq. (11). The time required to reach steady-state CO_2 concentration involves the addition of step 6 of Eq. (11). Steps 5 and 6 of Eq. (6) refer to exchange reactions of ^{18}O with the catalyst and do not enter into the reaction mechanism. Other plausible mechanisms could be written which would be consistent with the compartmental model corresponding to these equations.

One such mechanism which we assumed earlier (*29*) would be that step 2 in Eq. (6) is at equilibrium rather than unidirectional. This would switch chemisorbed carbidic carbon CI to the carbon monoxide pool COI, so that the first pool would be (CI + COI). The second pool of adsorbed species would then become CH_2I alone instead of

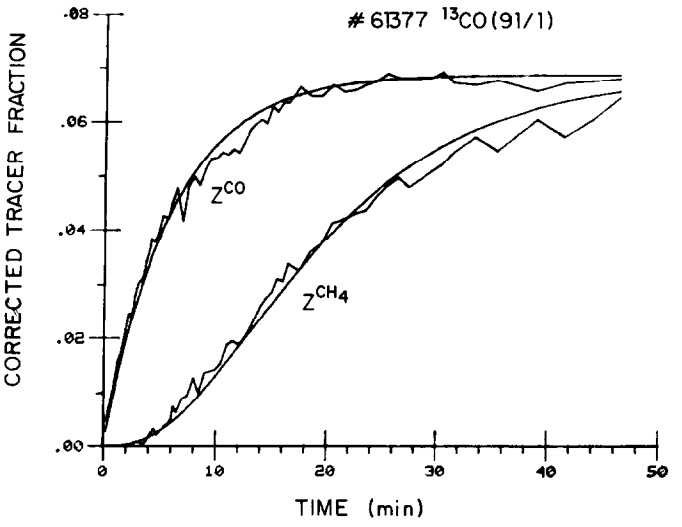

FIG. 6. ^{13}CO tracing: Ni catalyst. Smooth curve represents theoretical results. Uneven curve represents data. Run No. 61377; T = 175°C; feed molal ratio, H_2/CO = 91/1.

($Cl + CH_2l = CH_xl$) as in the present model. Data recently obtained by us indicate that once carbidic carbon is formed it does not exchange readily with the carbon in carbon monoxide during methanation so that this assumption seems to be untenable though it will fit the same compartmental model.

More complete deuterium tracing data will be needed to determine the nature of the CH_xl species on the catalyst surface. From the preliminary results obtained in Table 6 it appears that carbidic carbon, (i.e. $x = 0$), predominates. The formation of CH_2D_2 seems to be the next most abundant species, which may indicate the

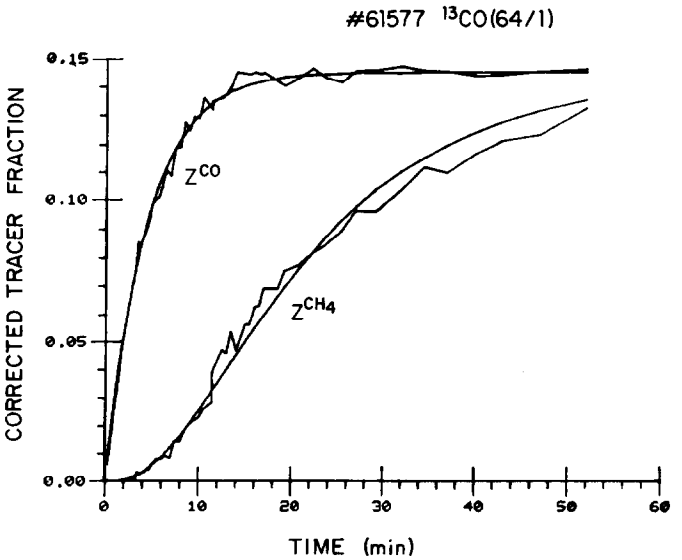

FIG. 7. ^{13}CO tracing: Ni catalyst. Smooth curve represents theoretical results. Uneven curve represents data. Run No. 61577; T = 176°C; feed molal ratio, H_2/CO = 64/1.

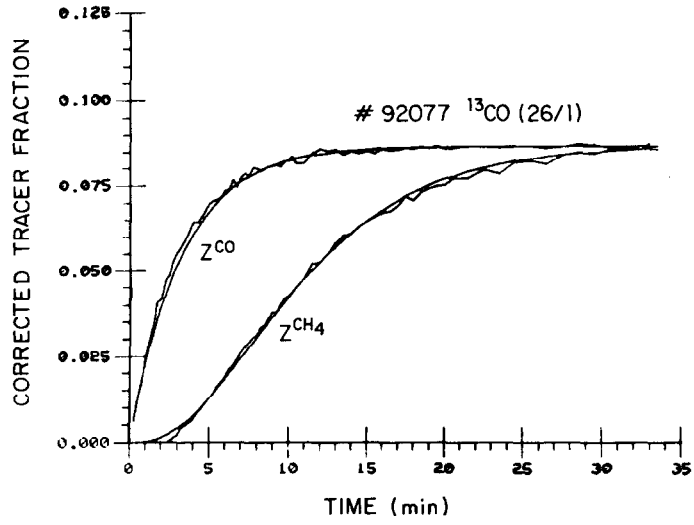

FIG. 8. ^{13}CO tracing: Ni catalyst. Smooth curve represents theoretical results. Uneven curve represents data. Run No. 92077; T = 220°C; feed molal ratio H_2/CO = 26/1.

addition of H_2 rather than atomic H. We chose to simply represent hydrogen as H_2 in Eqs. (6) and (11) until more data are available as to the mode of addition. Since hydrogen is not traced in the ^{18}O or ^{13}C experiments this simplification does not affect the interpretation we have made.

The possibility that a large concentration of fully hydrogenated CH_4l species is present on the catalyst during methanation is small. In the experiment described in Table 6, no CH_4 could be detected in the product after CH_4 had been flushed from the system. Also the extent of adsorption of methane on nickel is very small (*30*).

The calculated concentration of CH_xl

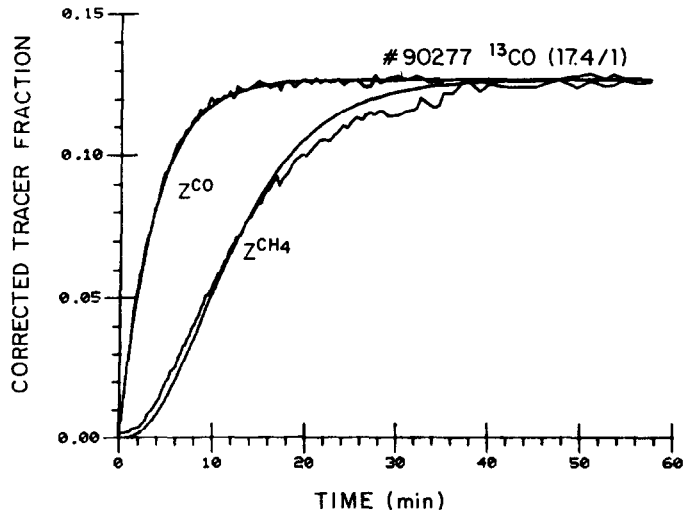

FIG. 9. ^{13}CO tracing: Ni catalyst. Smooth curve represents theoretical results. Uneven curve represents data. Run No. 90277; T = 217°C; feed molal ratio H_2/CO = 17/1.

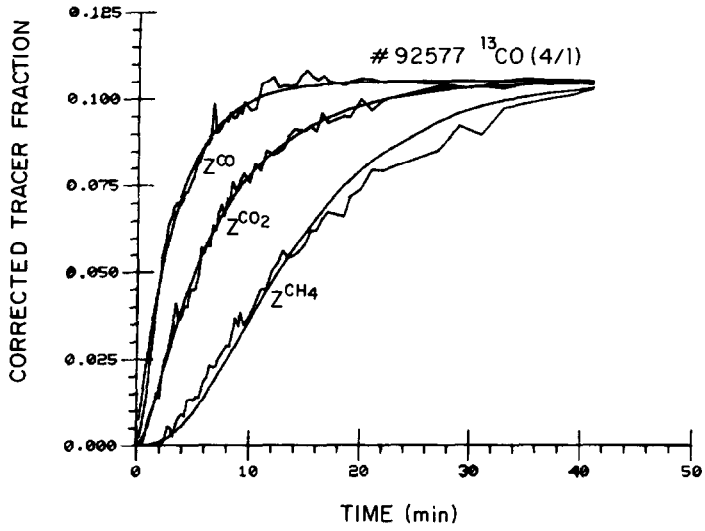

FIG. 10. ^{13}CO tracing: Ni catalyst. Smooth curve represents theoretical results. Uneven curve represents data. Run No. 92577; T = 258°C; feed molal ratio H_2/CO = 4/1.

generally does not exceed 4 ml/g of catalyst. At full monolayer coverage of these species this would correspond to each molecule of adsorbed CH_xI occupying about 3.5 surface sites (a monolayer of hydrogen corresponds to 7.1 ml/g of catalyst and occupies two surface sites per hydrogen molecule).

Further data are being obtained including experiments in which products as well as reactants are traced. This will serve to extend the preliminary conclusions reported here. Meanwhile the present results serve to illustrate the versatility of this technique. It furnishes more information than kinetic studies without isotopic tracing. The findings that an important rate-controlling step involves hydrogenation rather than only formation of carbidic carbon and that carbon dioxide is pro-

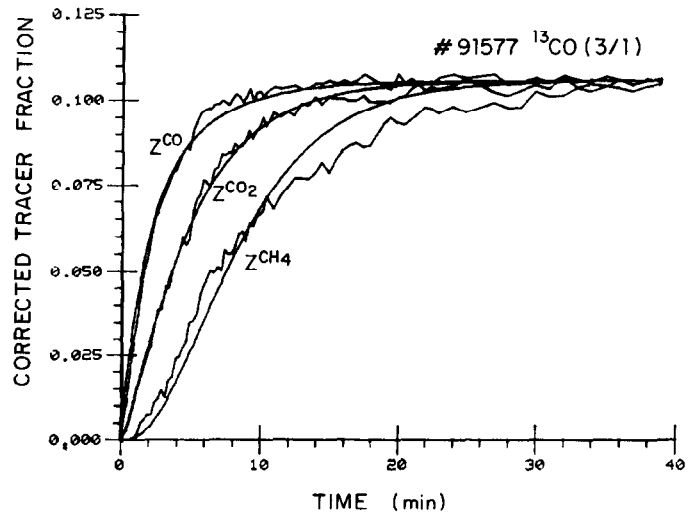

FIG. 11. ^{13}CO tracing: Ni catalyst. Smooth curve represents theoretical results. Uneven curve represents data. Run No. 91577; T = 276°C; feed molal ratio H_2/CO = 3/1.

duced directly rather than via the water gas shift mechanism provide increased understanding of the catalytic methanation reaction.

ACKNOWLEDGMENT

The authors are grateful for support of these studies by the National Science Foundation under Grant NSF-ENG 78-04055.

REFERENCES

1. Happel, J., *Catal. Rev.* **6** (2), 221 (1972).
2. Happel, J., and Hnatow, M. A., *Ann. N. Y. Acad. Sci.* **213**, 206 (1973).
3. Happel, J., Kiang, S., Spencer, J. L. Oki, S., and Hnatow, M. A., *J. Catal.* **50**, 429 (1977).
4. Berman, M., *Ann. N. Y. Acad. Sci.* **108**, 182 (1963).
5. Berman, M., *in* Laughlin and Webster, Eds.), "Advances in Medical Physics" pp. 199–296. Second International Conference on Medical Physics, Inc., Boston, 1971.
6. Berman, M., *Progr. Biochem. Pharmacol.* **15**, 92 (1978).
7. LeCardinal, G., Walter, E., Bertrand, P., Zoulalion, A., and Gelas, M., *Chem. Eng. Sci.* **32**, 733 (1977).
8. Happel, J., *Chem. Eng. Sci.* **33**, 1567 (1978).
9. LeCardinal, G., *Chem. Eng. Sci.* **33**, 1568 (1978).
10. Mezaki, R. and Happel, J., *Catal. Rev.* **3**, 241 (1969).
11. Froment, G. F., *AIChE J.* **21**, 1041 (1975).
12. Mills, G. A., and Steffgen, F. W., *Catal. Rev.* **8**, 159 (1973).
13. Vannice, M. A., *Catal. Rev. Sci. Eng.* **14**, 153 (1976).
14. Ponec, V., *Catal. Rev. Sci. Eng.* **18**, 151 (1978).
15. Blyholder, G., and Neff, L. D., *J. Phys. Chem.* **66**, 1664 (1962).
16. Dalla Betta, R. A., and Shelef, M., *J. Catal.* **48**, 111 (1977).
17. Ekerdt, J. G., and Bell, A. T., *J. Catal.* **58**, 170 (1979).
18. King, D. L., *Prepr. Amer. Chem. Soc. Div. Petrol. Chem.* **23** (2), 482 (1978).
19. Conrad, H., Ertl, G., Küppers, J., and Latta, E. E., *in* "Proceedings, 6th International Congress on Catalysis, London, 1976" (G. C. Bond, P. B Wells, and F. C. Tompkins, Eds.), p. 427 and discussion. The Chemical Society, London, 1977.
20. Araki, M., and Ponec, V., *J. Catal.* **44**, 439 (1976).
21. Wentrcek, P. R., Wood, B. J., and Wise, H., *J. Catal.* **43**, 363 (1976).
22. Dalmon, J. A., and Martin, G. A., *J. Chem. Soc. Faraday Trans. 1* **75**, 1011 (1979).
23. Rabo, J. A., Risch, A. P., and Poutsma, M. A., *J. Catal.* **53**, 295 (1978).
24. Happel, J., Odanaka, H., and Rosche, Paul, *AIChE Symp. Ser.* **67**, No. 115, 60 (1971).
25. Hayward, D. O., and Trapnell, B. M. W., "Chemisorption," 2nd. ed., p. 238, Butterworths, Washington, D.C., 1964.
26. Goodman, D. W., Kelley, R. D., Madey, T. E., and Yates, J. T., Jr., *in* "Advances in Chemistry Series" Vol. 178, p. 1. Amer. Chem. Soc., Washington, D.C., 1979.
27. Matsumoto, H., and Bennett, C. O., *J. Catal.* **53**, 331 (1978).
28. Imperial Chemical Industries, "Catalyst Handbook," pp. 190, 192. Springer-Verlag, New York, 1970.
29. Happel, J., Fthenakis, V., Suzuki, I., Yoshida, T., and Ozawa, S., Paper A37, "Seventh International Congress on Catalysis, Tokyo," 1980.
30. Frennet, A., *Catal. Rev. Sci. Eng.* **10** (1), 37 (1974).